Plant Physiology Preview. Published on February 24, 2010, as DOI:10.1104/pp.109.150946

Running head: AtNRAMP3 and AtNRAMP4 function in vacuolar Mn export (53 characters)

Corresponding author:
Sébastien Thomine
Institut des Sciences du Végétal, CNRS, Avenue de la Terrasse, 91198 Gif-sur-Yvette, France
Tel : +33 1 69 82 37 93
thomine@isv.cnrs-gif.fr

Journal research area
Environmental Stress and Adaptation

Title: Export of vacuolar manganese by AtNRAMP3 and AtNRAMP4 is required for optimal photosynthesis and growth under manganese deficiency

Authors:

Viviane Lanquar[1]*, Magali Schnell Ramos[1], Françoise Lelièvre[1], Hélène Barbier-Brygoo[1], Anja Krieger-Liszkay[2], Ute Krämer[3], Sébastien Thomine[1]†

1 Institut des Sciences du Végétal, CNRS, Avenue de la Terrasse, 91198 Gif-sur-Yvette, France

2 Service de Bioénergétique Biologie Structurale et Mécanismes (SB2SM), iBiTec-S, CEA Saclay, 91191Gif-sur-Yvette, France

3 University of Heidelberg, BIOQUANT 23, Im Neuenheimer Feld 267, D-69120 Heidelberg, Germany

This work was funded by the CNRS and ANR grant DISTRIMET (ANR-07-3-18-8487). VL received a PhD fellowship from the French ministry of research (ED 145). UK acknowledges a Heisenberg fellowship (Kr1967/4-1).

* present address: Carnegie Institution for Science, Department of Plant Biology, 260 Panama Street, Stanford CA 94 305, USA

†For correspondence: thomine@isv.cnrs-gif.fr

Abstract:

(201 words)

Manganese is an essential element, acting as cofactor in numerous enzymes. In particular, a Mn cluster is indispensable for the function of the oxygen evolving complex of photosystem II. Metal transporters of the natural resistance associated macrophage protein (NRAMP) family have the ability to transport both iron and manganese. AtNRAMP3 and AtNRAMP4 are required for iron mobilization in germinating seeds. The results reported here show that, in adult *Arabidopsis thaliana* plants, AtNRAMP3 and AtNRAMP4 have an important role in Mn homeostasis. Vacuolar Mn accumulation in mesophyll cells of rosette leaves of adult *nramp3nramp4* double mutant plants was dramatically increased when compared to wild type. This suggests that a considerable proportion of the cellular Mn pool passes through the vacuole and is retrieved in an AtNRAMP3/AtNRAMP4-dependent manner. The impaired Mn release from mesophyll vacuoles of *nramp3nramp4* double mutant plants is associated with reduced growth under Mn deficiency. However, leaf AtNRAMP3 and AtNRAMP4 protein levels are unaffected by Mn supply. Under Mn deficiency, *namp3nramp4* plants contain less functional photosystem II than the wild type. These data are consistent with a shortage of Mn to produce functional photosystem II, whereas mitochondrial Mn dependent superoxide dismutase (SOD) activity is maintained under Mn deficiency in both genotypes. The results presented here suggest an important role for AtNRAMP3/AtNRAMP4-dependent Mn transit through the vacuole prior to the import into chloroplasts of mesophyll cells.

Introduction

The catalytic centers of numerous enzymes rely on the ability of some transition metals to undergo changes in their redox state. Although Mn is involved as a cofactor in a range of additional biochemical pathways, the primary effect of Mn deficiency in photosynthetic organisms is a drop in photosynthetic activity (Marschner, 1995). The process of water splitting and oxygen evolution by photosystem II (PS II), which is a central component of oxygenic photosynthesis, requires a tetra-Mn cluster.

In plants, few of the mechanisms that enable the uptake, distribution, and storage of Mn have been characterized at the molecular level. Hyperpolarisation-activated Ca^{2+} channels and members of the ZIP family have been proposed as pathways for Mn uptake in roots (Korshunova et al., 1999; Vert et al., 2002; White et al., 2002; Pedas

et al., 2008). However, to our knowledge, no transporter specifically functioning in Mn uptake from soils has been reported in the root plasma membrane.

Most of the current knowledge on Mn compartmentation in plant cells comes from the analysis of the mechanisms of tolerance to Mn excess. Indeed, when accumulated in excess, Mn can be toxic and has been proposed to be sequestered in vacuoles and Golgi vesicles under these conditions (Marschner, 1995; Pittman, 2005). The analysis of the molecular mechanisms of Mn tolerance in *Stylosanthes hamata*, a tropical legume tolerant to high Mn led to the cloning of the Mn specific transport protein ShMTP8 (Delhaize et al., 2003). When expressed in Arabidopsis, ShMTP8 is targeted to the vacuolar membrane and confers Mn tolerance by mediating the sequestration of excess Mn in this compartment. In Arabidopsis, several pathways for Mn import into the vacuole have been identified. AtCAX2 and AtCAX4 Ca^{2+}/H^{+} antiporters are able to transport Mn into the vacuole (Hirschi et al., 2000; Pittman et al., 2004; Koren'kov et al., 2006). In addition, AtVIT1 increases the Mn content of the vacuoles when expressed in yeast (Kim et al., 2006). AtVIT1 is thus a good candidate to mediate Mn import into vacuoles. Recently, the functional analysis of AtMTP11 and PtMTP11, the homologues of ShMTP8 in Arabidopsis and poplar, suggested the existence of an alternative pathway for Mn detoxification by vesicle-mediated transport of this metal (Delhaize et al., 2007; Peiter et al., 2007). In addition, over expression of the Mn transporting P_{2A}-type ATPase, *AtECA1*, localized to the endoplasmic reticulum, increased Mn tolerance (Wu et al., 2002). Whether the vacuole represents an important site for the storage of Mn in plants grown under normal conditions is currently unknown. Moreover, little is known about the mechanisms involved in plant tolerance to Mn deficiency.

Recent work on barley confirmed an important decrease in the abundance of functional photosystem II under Mn deficiency and revealed differences in the fluorescence induction kinetics and state transitions between Mn efficient and inefficient genotypes (Husted et al., 2009). In barley, Mn deficiency also leads to increased water loss, likely through alteration of the leaf cuticle (Hebbern et al., 2009). Interestingly, in *C. reinhardtii*, another photosynthetic organism, in addition to causing a decrease in functional PS II abundance, Mn deficiency also impairs Mn dependent superoxide dismutase activity, leading to an increased sensitivity to oxidative stress (Allen et al., 2007). The cellular pathways for Mn transport and use under Mn deficient conditions are mostly unknown. A recent study on the Mn

transporting P_{2A}-type ATPase, *AtECA3*, localized to the Golgi apparatus, demonstrated the importance of Mn import into the Golgi apparatus under Mn deficiency (Mills et al., 2008).

NRAMPs represent another protein family likely to be involved in Mn transport in plants. Most NRAMP proteins characterized so far are able to transport a broad range of metals: Fe^{2+}, Mn^{2+}, Zn^{2+}, Cd^{2+} [for review: (Colangelo and Guerinot, 2006; Nevo and Nelson, 2006)]. In bacteria, NRAMP homologues, MntH, function primarily as cellular Mn uptake transporters (Makui et al., 2000). Moreover, *MntH* gene expression is regulated at the transcriptional level through MntR, a Mn-sensing regulatory protein (Que and Helmann, 2000; Patzer and Hantke, 2001). In *C. reinhardtii, NRAMP1* is up-regulated upon Mn deprivation (Allen et al., 2007). In yeast, NRAMP homologues, Smf1p and Smf2p, are involved in Mn uptake and recycling. They are co-regulated at the post-translational level by this metal (Liu and Culotta, 1999; Portnoy et al., 2000). The disruption of *SMF2* leads to the loss of activity of the mitochondrial Mn superoxide dismutase (SOD) and of Golgi Mn-dependent enzymes (Luk and Culotta, 2001).

In Arabidopsis, six members of the NRAMP family have been identified. Heterologous expression of the *AtNRAMP1*, *3* and *4* cDNAs in yeast mutants deficient for metal uptake, indicated that these proteins are able to transport Fe, Mn and Cd (Curie et al., 2000; Thomine et al., 2000). AtNRAMP3-GFP and AtNRAMP4-GFP fusion proteins are targeted to the vacuolar membrane (Thomine et al., 2003; Lanquar et al., 2005). In addition, AtNRAMP4 was identified in the vacuolar proteome of Arabidopsis mesophyll cells (Carter et al., 2004). *AtNRAMP3* and *AtNRAMP4* are strongly expressed during the early stages of germination and the *nramp3nramp4* double mutant displays a strong chlorotic phenotype when seeds are germinated in the absence of Fe supply in the medium (Lanquar et al., 2005). It was thus proposed that AtNRAMP3 and AtNRAMP4 play redundant roles in export of Fe from the vacuole during seed germination. In the present study, a detailed examination of the *nramp3nramp4* double mutant adult plants indicated that AtNRAMP3 and AtNRAMP4 crucially contribute to Mn homeostasis. AtNRAMP3 and AtNRAMP4 are required for Mn mobilization from the vacuole of mesophyll cells in adult plants. As a consequence, *nramp3nramp4* over-accumulate Mn in vacuoles under standard growth conditions, and *nramp3nramp4* growth is strongly impaired under Mn deficiency. This growth phenotype is associated with a decrease in the number of

functional PSII attributable to a shortage of Mn clusters, whereas mitochondrial Mn SOD activity is maintained. The results presented show that AtNRAMP3 and AtNRAMP4 play a major role in the export of vacuolar Mn in photosynthetic tissues of adult plants. These results highlight the importance of Mn transit through vacuoles en route to its main usage site in chloroplasts.

Results

AtNRAMP3 and AtNRAMP4 are involved in Mn retrieval from the vacuole of mesophyll cells

To gain insight into the function of AtNRAMP3 and AtNRAMP4 in adult plants, the consequences of their absence were investigated in mesophyll cells from plants grown on soil for 6 weeks.

Intact mesophyll protoplasts were released from rosette leaves and subsequently, the mesophyll protoplast preparation was subjected to gentle lysis and intact vacuoles were recovered. Microscopic observation of the protoplast preparation revealed that only mesophyll protoplasts were present, no other cell types could be recognized and that the vacuole preparation was of high purity. Furthermore, vacuolar pyrophosphatase (V-PPase), a vacuolar membrane protein, was enriched in the vacuole preparation in comparison to the protoplast from which they were extracted (Figure 1A), whereas E37, a chloroplast envelope protein was not detected (data not shown) (Ferro et al., 2002).

AtNRAMP3 and AtNRAMP4 protein levels were examined in leaves, mesophyll protoplasts and vacuoles by immunoblot using isoform specific antibodies (Figure S1) (Lanquar et al., 2005). In *nramp3nramp4* leaves, protoplasts or vacuoles, no signal corresponding to AtNRAMP3 or AtNRAMP4 was detected (Figure 1A), confirming the absence of both proteins. In wild-type plants, AtNRAMP3 and AtNRAMP4 were detected in leaves and in mesophyll protoplasts. There was only a weak signal for AtNRAMP3 in mesophyll protoplasts. This indicates that AtNRAMP3 may be more abundant in other leaf tissues, such as the vasculature, than in mesophyll, in agreement with *AtNRAMP3* expression pattern (Thomine et al., 2003). In mesophyll vacuoles, the signals corresponding to AtNRAMP3 and AtNRAMP4 were about 20 times stronger than in mesophyll protoplasts, indicating an enrichment of these two membrane proteins (Figure 1A). These results indicate that both AtNRAMP3 and AtNRAMP4 are localized in the vacuolar membrane of mesophyll

cells of adult leaves as previously reported in other cell types (Thomine et al., 2003; Lanquar et al., 2005).

To investigate the functions of AtNRAMP3 and AtNRAMP4 in mesophyll cells, the metal concentrations were measured by ICP-AES in leaf tissues, mesophyll protoplasts and mesophyll vacuoles of wild-type and *nramp3nramp4* plants grown on soil. The concentrations of iron, manganese and zinc, three possible substrates of NRAMP3 and NRAMP4, were similar in *nramp3nramp4* and wild-type leaves (Figure 1B). This result is consistent with published data on younger seedlings (Lanquar et al., 2005). Similarly, no statistically significant differences were observed between metal contents of *nramp3nramp4* and wild-type mesophyll protoplasts for Fe, or Zn (Figure 1B). By contrast, protoplasts isolated from *nramp3nramp4* plants contained 2.1 to 2.8 more Mn than wild-type protoplasts (Figure 1B). Furthermore, analysis of *nramp3nramp4* vacuoles revealed that they contained between 6.5 and 56 times more Mn than wild-type vacuoles (Figure 1B). An additional experiment employing an independent *nramp3nramp4* double knockout mutant in the Columbia accession confirmed the strongly increased vacuolar Mn content in *nramp3nramp4* double mutants when compared to the wild type (Ravet et al., 2009b). Microscopic observations did not show any size difference between wild-type and *nramp3nramp4* double mutant vacuoles. Furthermore, no statistically significant difference in vacuolar contents of Fe or Zn was detected between the double mutant and the wild type.

These results show that the loss of AtNRAMP3 and AtNRAMP4 proteins greatly enhances the sequestration of Mn in mesophyll vacuoles, while in wild-type plants, AtNRAMP3 and AtNRAMP4 continuously mediate the retrieval of Mn from the vacuole. Furthermore, these results suggest that net Mn storage in the vacuole of mesophyll cells is minor in wild-type *A. thaliana* under normal growth conditions (about 10% of protoplast Mn), but that a substantial proportion of cellular Mn transits through the vacuole.

Adult *nramp3nramp4* plants display a conditional growth defect under Mn deficiency

The results of this study indicate that in *nramp3nramp4* mesophyll cells, Mn sequestration in the vacuole is strongly increased. To test whether this alteration in intracellular Mn distribution is associated with a defect in plant growth, plants were grown on perlite and watered either with a control Mn-sufficient nutrient solution

containing 5 µM Mn (C) or with a nutrient solution lacking Mn (Mn-deficient conditions, - Mn). After 9.5 weeks of growth, the biomass of *nramp3nramp4*, *nramp3* and *nramp4* mutant rosettes grown under control conditions was not significantly different from that of wild-type plants (Figure 2A, C, D and Table I). The rosettes of adult *nramp3nramp4* mutant appeared smaller because their leaves were curled: the leaf margins grow towards the abaxial side of the leaf (Figure 2A, B). The effect of Mn deficiency on wild type was variable between different experiments: wild-type rosette biomass was not reduced in the experiment displayed in Figure 2C and reduced by 45% compared to control conditions in the experiments shown in Figure 2D and Table I. By contrast, *nramp3nramp4* consistently displayed a much stronger growth reduction than wild type under Mn deficient conditions (63% in Figure 2C to 86% in Figure 2D, n = 4 independent biological replicates; Table I). Qualitatively similar results were obtained in hydroponic culture (Figure S3A). Under Mn deficiency, *nramp3nramp4* mutant leaves were not curled but their size was reduced in comparison with wild type (Figure 2B). The rosette biomass of *nramp3* and *nramp4* single mutants was indistinguishable from the wild type (Figure 2C), indicating that AtNRAMP3 and AtNRAMP4 are functionally redundant under Mn-deficient conditions. Measurements of dry biomass gave comparable results indicating that the water content was similar between wild-type, *nramp3*, *nramp4* and *nramp3nramp4* plants grown either under control conditions or under Mn deficiency (data not shown). The growth phenotype of the *nramp3nramp4* mutant under Mn deficiency could be rescued by introduction of *AtNRAMP3* or *AtNRAMP4* wild-type genes in the *nramp3nramp4* mutant background (Figure 2D and S2).

The growth defect of the *nramp3nramp4* mutant is not associated with reduced Mn concentrations in leaves or mesophyll protoplasts

To test whether the lower growth of *nramp3nramp4* mutants under Mn deficiency is associated with a decreased Mn content in leaves or mesophyll cells, metal concentrations in leaves and metal contents of mesophyll protoplasts were measured by ICP-AES in plants grown on perlite under controlled mineral nutrition. Plants were watered either with control Mn-sufficient nutrient solution (C) or with a nutrient solution lacking Mn (- Mn). Upon growth under control conditions, no differences in leaf metal concentrations were observed between wild-type and *nramp3nramp4* mutant plants for Fe, Mn and Zn (Figure 3A). In wild-type and *nramp3nramp4* mutant plants, growth under Mn deficient conditions resulted in a decrease in leaf Mn

concentrations by about 90% when compared to plants grown under control conditions; in wild-type plants grown under Mn-deficient conditions, Fe concentrations were unchanged and Zn concentrations were slightly increased (Figure 3A). Fe, Mn and Zn concentrations in leaves of the *nramp3nramp4* mutant grown under Mn-deficient conditions were significantly higher than in leaves of the wild type in the same conditions. No statistically significant differences were detected between either *nramp3* or *nramp4* single mutant and wild-type rosette metal concentrations for any of the three metals Fe, Mn or Zn (Table SI).

For Fe and Zn, relative metal concentrations in mesophyll protoplasts isolated from plants grown under control or Mn deficient conditions followed a similar pattern as leaf metal concentrations (Figure 3B, left and right panel). Mn concentrations in *nramp3nramp4* mutant protoplasts were 2 to 3-fold higher than in wild-type protoplasts under control (Mn- sufficient) conditions. This result is in agreement with the result obtained on mesophyll protoplasts from plants grown on soil (Figure 1B). In contrast, under Mn deficiency, relative Mn concentrations in wild-type and *nramp3nramp4* mutant protoplasts were not statistically different (Figure 3B).

Taken together, these data demonstrate that Mn concentrations in *nramp3nramp4* leaves or mesophyll protoplasts, respectively, are equal or higher than in the wild type, under both control and Mn deficient conditions. This result excludes that a defective Mn supply to *nramp3nramp4* mesophyll cells is responsible for the growth defect of this mutant under Mn deficiency.

The level of active Photosystem II is lower in *nramp3nramp4* mutant under Mn deficiency

Manganese is an essential cofactor of the water splitting complex of photosystem II (PS II). Therefore, the growth defect observed in *nramp3nramp4* under Mn-deficient conditions could be explained by a defect in the ability to split water, leading to a lower activity of photosynthesis. Since a defect in PS II can be detected through the quantification of chlorophyll fluorescence, the ratios Fv/Fm were measured in wild-type and *nramp3nramp4* plants (Maxwell and Johnson, 2000).

Ratios Fv/Fm close to 0.8 obtained for wild-type, *nramp3*, *nramp4* and *nramp3nramp4* plants grown under control (Mn sufficient) conditions are consistent with ratios reported for *Arabidopsis thaliana* and other higher plants (Björkman and Demmig, 1987)(Table I and SII, Figure S4). In Mn deficient plants, the ratio dropped to 0.65 for wild-type plants and was further significantly reduced to 0.57 in the

nramp3nramp4 plants (Table I). This indicates a decline of the photosynthetic efficiency under Mn deficiency, which is exacerbated in the *nramp3nramp4* mutant compared to the wild type. Fv/Fm ratios were rescued to values equal or higher than wild type in *nramp3nramp4* mutant lines complemented by *AtNRAMP3* or *AtNRAMP4* (Table SII). In the same conditions, Fv/Fm ratios in *nramp3* and *nramp4* single mutants, respectively, were not significantly lower than in the wild type, confirming the functional redundancy of these two genes (Figure S4). Upon prolonged growth in Mn deficient conditions for an additional 3 weeks, Fv/Fm ratio dropped to similarly low values for wild type, *nramp3*, *nramp4* and *nramp3nramp4* (Figure S4).

To further investigate the effect of Mn deficiency on PSII, thermoluminescence measurements were performed on intact leaves of plants grown under Mn deficient and sufficient conditions on perlite for 8 weeks. In thermoluminescence measurements, the emitted light originates from charge recombinations of trapped charge pairs within PS II (Inoue, 1996). The charge pairs involved can be identified by their emission temperature, which strongly depends on the redox potentials of the charge pairs. The most important thermoluminescence band for investigating the electron transfer within PSII is the B-band. Recombination of S_2 or S_3 state of the oxygen-evolving complex at the donor side of PSII with the semi-reduced secondary quinone acceptor in PSII, Q_B^-, yields the B-band at around 30°C (Rutherford et al., 1982). Figure 4A shows the changes in the intensity of the B-band at 24°C recorded from leaves of dark-adapted plants in dependence on the number of exciting single turnover flashes. As expected for leaves, the highest intensity of the B-band was observed after the second flash and the intensity of this band oscillates with a period of 4. This oscillation reflects the cycle of the oxidation states of the Mn cluster (S_{0-4}) (Figure 4A). In *nramp3nramp4* leaves, the intensity of the B-band was strongly reduced. A normal oscillation pattern was still observed during the first four flashes. This was dampened almost completely when more flashes were given (Figure 4A). These results show that the function of the water-splitting complex is normal in *nramp3nramp4*, but that only very few Mn clusters are functional in the *nramp3nramp4* double mutant. A low intensity of the flash-induced B-band has been described previously in tobacco plants in which the level of PsbP was severely down-regulated by the RNA interference technique. In these plants the Mn cluster of PSII is very unstable and disassembles quickly in the dark (Ifuku et al., 2005).

In Mn deficient *nramp3nramp4* plants, PS II was highly susceptible to illumination with high light (Figure 4B). When leaves of Mn-deficient *nramp3nramp4* plants were exposed to high light intensities (2000 µmol quanta m^{-2} s^{-1}) for 1 h, the variable fluorescence was lowered to values below the fluorescence level measured with the low intensity measuring light on dark adapted leaves (Figure 4B, upper left panel). This indicates that the plastoquinone pool was partially reduced in the dark-adapted plants prior to the measurements (Bondarava et al., 2003). During a subsequent period of incubation in dim light for 3 h, the variable fluorescence probed by short flashes of actinic light did not recover, suggesting that the repair of photoinhibited PS II was not achieved. In the presence of Mn, the mutant showed a much lower loss of variable fluorescence (lower left panel), and the recovery of the variable fluorescence was similar to that of wild type grown under identical conditions (lower right panel).

The level of D1 (PsbA), the core protein of PS II which binds the Mn cluster, was analyzed by immunoblotting in wild-type and *nramp3nramp4* leaves from plants grown under control and Mn deficient conditions. In plants grown under Mn sufficient conditions D1 protein levels were higher in *nramp3nramp4* than in wild-type leaves (Figure 4C and S5). The amount of D1 was strongly reduced in Mn deficient wild-type leaves, and even further reduced in Mn-deficient *nramp3nramp4* mutant plants (Figure 4C and S5). The decreased abundance of D1 protein in Mn deficient *nramp3nramp4* mutant leaves is in agreement with the observation of a lower number of active PS II in these plants (Table 1, Figure S4).

The growth defect observed in the mutant under Mn deficiency is thus associated with a severe decrease in the number of functional PS II centers. To test whether the decrease in the number of functional PS II is associated with a shortage of Mn, we measured the relative Mn concentrations in chloroplasts isolated from mesophyll cells of wild-type and *nramp3nramp4* plants grown under control and Mn deficient conditions. Relative Mn concentrations were similar in chloroplasts from wild type and *nramp3nramp4* grown under control conditions. The Mn concentrations in chloroplasts of Mn-deficient wild-type plants was reduced to 50% of that of control plants (Figure 4D). Under Mn deficiency, *nramp3nramp4* mutant chloroplasts exhibited merely about half of the Mn concentration found in wild type. This result suggests that a reduced availability of Mn to form Mn clusters in the chloroplasts is a

cause of the lower number of active PS II in the mutant under Mn deficiency. Taken together, these data indicate that under Mn deficiency, the defect in Mn export from the vacuole in *nramp3nramp4* perturbs Mn allocation to the chloroplast and leads to a lower number of active PS II.

Manganese dependent Superoxide Dismutase activity is not reduced in *nramp3nramp4* mesophyll cells

As the defect in Mn export from the vacuoles of *nramp3nramp4* reduces the number of functional PS II in leaves under Mn deficiency, we tested whether the function of the other quantitatively major Mn-dependent protein, MnSOD, is defective in this mutant. In-gel measurements of SOD activity were performed after separation by native PAGE of total protein extracts from leaves of wild type and *nramp3nramp4* mutants grown on perlite under control conditions, Fe deficiency or Mn deficiency. Three bands were detected that displayed SOD activity (Figure 5A). On the basis of inhibition by KCN (not shown) and H_2O_2 (Figure 5B), the bands could be assigned to CuZnSOD (KCN and H_2O_2 sensitive), FeSOD (H_2O_2 sensitive) and MnSOD (insensitive to KCN and H_2O_2). Under Fe deficiency, FeSOD activity was strongly reduced in both wild-type and *nramp3nramp4* mutant leaves (Figure 5A). Under Mn deficiency, MnSOD was neither strongly decreased in the wild type nor in the *nramp3nramp4* double mutant (Figure 5B). These data show that in contrast to PS II function, MnSOD activity, which is known to be localized in the mitochondria, is maintained in the *nramp3nramp4* mutant under Mn deficiency.

Regulation of AtNRAMP3 and AtNRAMP4 protein levels

Previous results indicated that in seedlings, AtNRAMP3 and AtNRAMP4 expression levels are regulated in response to Fe status (Thomine et al., 2003; Lanquar et al., 2004; Lanquar et al., 2005). The results obtained in the present study suggested an important role of AtNRAMP3 and AtNRAMP4 in Mn distribution to PS II under Mn deficiency. Therefore, the regulation of AtNRAMP3 and AtNRAMP4 protein levels was reexamined in adult plants grown under Fe or Mn deficient conditions. Wild-type and *nramp3nramp4* plants were grown hydroponically under control (C), Fe deficient (- Fe) and Mn deficient (- Mn) conditions. In Fe-deficient plants, Fe concentrations were decreased by 85% in shoots and 90% in roots of both genotypes when compared to controls (Figure S3B) while Mn accumulation was increased as previously described (Vert et al., 2002). In Mn-deficient plants, Mn concentrations were decreased by 90% in shoots and 80% in roots when compared to controls

(Figure S3B). Concentrations of other cations were unchanged. AtNRAMP3 and AtNRAMP4 protein levels were analyzed by immunoblot in 3 biological replicates. Under Fe deficiency, AtNRAMP3 protein levels increased in roots (in 2 out of 3 experiments) but did not show any regulation in shoots of adult plants (Figure 6A). Levels of AtNRAMP4 protein increased under iron deficiency in both shoots (in 3 out of 3 experiments) and roots (in 2 out of 3 experiments). These results are consistent with previous reports (Thomine et al., 2000; Lanquar et al., 2005). In contrast, these experiments did not reveal any significant regulation of AtNRAMP3 or AtNRAMP4 protein levels in response to Mn deficiency (Figure 6A). In addition, staining of promoter AtNRAMP3::GUS (Thomine et al., 2003) or promoter AtNRAMP4::GUS (Lanquar et al., 2005) seedlings grown for 7 days on agar based medium containing either no Mn (- Mn) or 0.1 mM Mn (control) did not exhibit any Mn-dependent regulation of *AtNRAMP3* or *AtNRAMP4* promoter activity (data not shown and Lanquar et al. 2005).

Ferritin protein levels are up-regulated in *nramp3nramp4* mutants under Mn deficiency

The specific up-regulation of AtNRAMP3 and AtNRAMP4 under Fe deficiency, although they are primarily involved in Mn mobilization from the vacuole in adult plants, is intriguing. To further investigate this apparent link between Fe and Mn homeostasis, the level of ferritin 1 protein, AtFER1, was monitored in leaves of wild-type and *nramp3nramp4* plants grown hydroponically under control, Mn-deficient (- Mn) and Fe-deficient (- Fe) conditions. Immunoblots to detect AtFER1 were performed on four independent biological replicates. Ferritins store Fe in non-toxic form in the stroma of chloroplasts (Briat et al., 1999). In plants grown under control conditions, the levels of AtFER1 in shoots were unchanged in the double mutant (in 3 out of 4 experiments) (Figure 6B). Under Fe deficiency, AtFER1 is neither detectable in the wild type nor in the double mutant (in all 4 experiments), as described previously (Ravet et al., 2009a). Under Mn deficiency, the amount of AtFER1 in wild-type plants was slightly decreased compared to the signal observed in control conditions (in 2 out of 4 experiments), or unchanged (in 2 out of 4 experiments). Interestingly, in Mn-deficient *nramp3nramp4* plants, the amount of ferritin 1 was consistently between 3.5 and 7 times higher when compared to wild type grown under the same conditions (in 4 out of 4 experiments; Figure 6B). This increase was consistently observed in plants grown in perlite watered with – Mn medium, in plants

grown hydroponically in - Mn medium and in two week-old-plants grown on Mn-deficient agar medium. The up-regulation of AtFER1, a component of Fe homeostasis in the shoots of *nramp3nramp4* mutants under Mn deficiency suggests a higher iron status in chloroplasts of *nramp3nramp4* mutants compared to wild type under these conditions. This is in agreement with the higher iron concentrations in leaves and protoplasts from Mn deficient *nramp3nramp4* compared to wild type (Figure 3).

To test whether other components of the Fe homeostasis network were also deregulated, the levels of AtFER1 and AtIRT1 were monitored in the roots. Protein extracts from 2 biologically independent replicates were analyzed. AtIRT1 is the high affinity Fe transporter, and IRT1 protein levels are up-regulated under Fe deficiency (Connolly et al., 2002; Seguela et al., 2008). IRT1 was detected only in roots of Fe-deficient plants and protein levels were equivalent in wild-type and *nramp3nramp4* plants (Figure 6B). This is different from the finding in barley, where HvIRT1 is up-regulated in response to both Fe and Mn deficiency (Pedas et al., 2008). AtFER1 protein levels were equivalent in roots of wild-type and *nramp3nramp4* plants under control and Mn deficient conditions (data not shown).

Discussion

The results presented in this study demonstrate that AtNRAMP3 and AtNRAMP4 are involved in Mn homeostasis in the adult plant. The strong accumulation of Mn in *nramp3nramp4* mutant mesophyll vacuoles suggests that in this tissue, AtNRAMP3 and AtNRAMP4 participate in the release of Mn from the vacuoles (Figure 1). Under Mn deficiency, *nramp3nramp4* double mutant plant growth is reduced (Figure 2). This growth defect correlates with a lower number of functional PS II, consistent with a shortage of Mn to form Mn clusters (Figure 3).

AtNRAMP3 and AtNRAMP4 operate in the retrieval of Mn from vacuoles in leaf mesophyll cells

Mesophyll vacuoles of adult *nramp3nramp4* plants contain substantially higher amounts of Mn than those of the wild type (Figure 2). This result suggests a function of AtNRAMP3 and AtNRAMP4 in the retrieval of Mn from vacuoles. Transfer of Mn into and retrieval from vacuoles thus appears to proceed continuously in the wild type, resulting in the accumulation of, on average, only 10% of protoplast Mn inside vacuoles in the steady state (Figure 1B). The results obtained here suggest that the

mesophyll vacuole is predominantly a compartment for Mn transit rather than for Mn storage. Despite the strongly enhanced accumulation of Mn in vacuoles of the *nramp3nramp4* mutant, global leaf Mn concentrations are barely increased when compared to the wild type (Figure 1, 3, S3). This could be due to the fact that the mesophyll intracellular Mn pool accounts for only a minor part of total leaf Mn. Mn concentrated in the cell wall or in other leaf cell types, such as vascular bundles or epidermal cells, could mask differences between the mesophyll cells of different genotypes. Alternatively, in the mutant, the increase in mesophyll vacuolar Mn contents could be compensated by a reduction in Mn contents in a different cell type. Lack of AtNRAMP3 and AtNRAMP4 leads to a modification of the subcellular distribution of Mn. While mesophyll vacuoles of wild-type plants grown on soil contain on average 10% of total Mn pool in mesophyll protoplasts, vacuoles isolated from the mutant contain on average 70% of the intracellular Mn. By contrast, 92% and 80% of the total protoplast Zn pool was associated with the vacuoles of wild-type and mutant mesophyll cells, respectively. The finding that only 10% of the Mn is associated with wild-type vacuoles is surprising in view of other studies indicating that most Mn is stored in the vacuole. Based on Mn broadening of ^{31}P NMR signal or on the analysis of ^{54}Mn radiotracer release kinetics, Quiquampoix et al. and Pedas et al. concluded that most Mn is stored in the vacuoles of maize and barley root cells, respectively (Quiquampoix et al., 1993; Pedas et al., 2005). The discrepancy with our results may be explained by the use of different experimental approaches or by a different intracellular distribution of Mn in root and mesophyll cells or by differences in Mn storage between species. González and Lynch reported that most Mn is stored in the vacuole of bean leaf cells (González and Lynch, 1999). However, their study addressed Mn storage under Mn excess, a condition in which vacuolar Mn sequestration may be favored.

Iron was also detected in mesophyll vacuoles of wild-type and double mutant plants. Although AtNRAMP3 and AtNRAMP4 are capable of Fe transport (Thomine et al., 2000; Lanquar et al., 2005), no difference between the Fe content of *nramp3nramp4* and wild-type vacuoles was detected (Figure 1), even when vacuoles were isolated from the mesophyll of Fe deficient plants (data not shown). Thus, AtNRAMP3 and AtNRAMP4 are not likely to be required for Fe export from the vacuole in this tissue. However, the relatively high variation between biological replicates could mask small

differences in Fe contents between wild-type and the *nramp3nramp4* double mutant vacuoles.

Under Mn deficiency, optimal Mn supply to chloroplasts requires AtNRAMP3/AtNRAMP4-dependent Mn transit through the vacuole

When plants are grown in control conditions, the high amount of Mn retained in *nramp3nramp4* vacuoles does not lead to any reduction in plant growth (Figure 2, S3). This suggests that, although a large proportion of cellular Mn transits through the vacuole in the mesophyll of wild-type plants, a lack of AtNRAMP3/AtNRAMP4-dependent Mn retrieval from the vacuole does not limit cellular Mn supply. However, under Mn deficiency, *nramp3nramp4* plants display a strong growth reduction (Figure 2). This growth inhibition is not associated with a lower Mn pool in mesophyll cells (Figure 3), but with an alteration of the intracellular distribution of Mn instead. Chloroplast Mn concentrations of Mn deficient *nramp3nramp4* plants were much lower than in wild-type plants (Figure 4). The intracellular Mn that is missing in the chloroplasts of *nramp3nramp4* plants is likely sequestered in the vacuoles, based on the results obtained using Mn sufficient plants (Figure 2). These results suggest that, under Mn deficiency, transit of Mn through the vacuole becomes a limiting pathway for the distribution of this metal to indispensable Mn-requiring proteins. Mn is an important cofactor of the oxygen-evolving complex of PS II. Compared to the wild type, a lower number of functional PS II correlated with an enhanced impact of Mn deficiency on biomass production in the double mutant. By contrast, mitochondrial MnSOD activity was not decreased under Mn deficiency in the wild type or in *nramp3nramp4*. The results presented suggest that under Mn deficiency, the use of the vacuolar Mn pool is required for optimal photosynthesis and plant growth but not for providing Mn cofactor to MnSOD in mitochondria. In contrast, in *C. reinhardtii*, Mn deficiency leads to a decrease in both PS II fluorescence and MnSOD activity (Allen et al., 2007). In Arabidopsis mesophyll cells, the oxygen evolving complex of PS II thus appears as a major Mn requiring enzyme, and its activity is more sensitive to Mn deficiency than that of MnSOD, in agreement with previous work on other plants (Marschner, 1995). In yeast, SMF2, a membrane protein of the NRAMP family localized in intracellular vesicles, plays a role in providing Mn to mitochondrial SOD (Luk and Culotta, 2001). In Arabidopsis, this role could be played by another Mn transport pathway distinct from AtNRAMP3 and AtNRAMP4. The results presented here underline the importance of Mn transit through the vacuole for Mn supply to the

chloroplast under conditions of Mn deficiency, whereas under Mn sufficient conditions Mn transit through the vacuole is not required to maintain the primary Mn-dependent chloroplast function. Under Mn deficiency, the cellular Mn uptake is strongly reduced due to low external availability, and we hypothesized that cellular Mn recycling following protein degradation becomes substantially more important. Cellular Mn recycling is likely to involve passage through the vacuole as a compartment known to be involved in organelle autophagy (Wada et al., 2009). We speculate that under Mn deficiency and non-excess Mn sufficiency, Mn transit through the vacuole is part of a continuous cellular recycling pathway for Mn involving AtNRAMP3 and AtNRAMP4, which becomes essential for the maintenance of photosynthesis and growth under conditions of Mn deficiency. However, as the results presented in Figure 1A do not formally exclude that AtNRAMP3 and AtNRAMP4 may reside on other membranes than the tonoplast, the possibility remains that *nramp3nramp4* phenotype is also related to a defect in Mn transport to or from another intracellular compartment.

AtNRAMP3 and AtNRAMP4 have redundant functions in mesophyll cells

Under Mn deficiency, decreases in plant biomass production and maximum quantum yield were only observed in the *nramp3nramp4* double mutant, and not in *nramp3* and *nramp4* single mutants (Figure 2, S4). This result indicates that *AtNRAMP3* and *AtNRAMP4* genes have redundant functions in Mn homeostasis in leaves. This is in agreement with previous reports on the redundant function of AtNRAMP3 and AtNRAMP4 in Fe mobilization during seed germination and in cadmium tolerance (Lanquar et al., 2005; Oomen et al., 2009). By contrast, AtNRAMP3 and AtNRAMP4 functions in pathogen resistance are additive (Segond et al., 2009). Overlapping, but not fully identical localization of *AtNRAMP3* and *AtNRAMP4* promoter activity (Thomine et al., 2003; Lanquar et al., 2005), and circumstantial evidence for a higher abundance of the AtNRAMP4 protein in mesophyll cells when compared to AtNRAMP3 (Carter et al., 2004) support both the possibility of functional redundancy as well as of functional differentiation between the two proteins.

Cross talk between Fe and Mn homeostasis

Although other NRAMP family members in yeast, *C. reinhardtii* and bacteria are up-regulated under Mn deficiency, neither AtNRAMP3 nor AtNRAMP4 is regulated in response to Mn deficiency at the protein level (Portnoy et al., 2000; Patzer and Hantke, 2001; Allen et al., 2007). It is possible that the expression level of

AtNRAMP3 and AtNRAMP4 observed under control conditions is sufficient to support sufficient rates of Mn retrieval from vacuoles also under Mn deficiency. Alternatively, the transport activity of these proteins might be regulated at a different level. In contrast, AtNRAMP3 and AtNRAMP4 protein abundance is up-regulated in response to Fe deficiency (Figure 6) (Lanquar et al., 2005). This suggests that AtNRAMP3 and AtNRAMP4 may play a role during iron deficiency in adult plants, which remains to be identified. Previous report showed that, in *nramp3* knockout mutants, Mn accumulation is increased under severe Fe deficiency (Thomine et al., 2003). Conversely, Mn accumulation under Fe deficiency is reduced in 35S-*AtNRAMP3* Arabidopsis lines (Thomine et al., 2003). This effect was associated with similar changes in Zn accumulation and other responses to Fe deficiency, suggesting that AtNRAMP3 modulates responses to Fe deficiency (Baxter et al., 2008). In the present study, no difference in Mn accumulation was detected between adult wild-type and *nramp3nramp4* plants grown under Fe deficiency (Figure S3). In *C. reinhardtii*, Mn deficiency leads to secondary iron deficiency (Allen et al., 2007). Under the conditions used in this study, none of the Arabidopsis Fe deficiency-responsive proteins analyzed, AtNRAMP3, AtNRAMP4 or IRT1, is up-regulated under Mn deficiency indicating that Mn deficiency does not trigger secondary Fe deficiency.

Increased accumulation of ferritin 1 and an increase in iron concentration in leaves of *nramp3nramp4* plants grown under Mn deficiency suggests a coordinated homeostasis of Mn and Fe (Figures 3, 6). It was shown that, in *C. reinhardtii*, Fer1 is up-regulated under iron deficiency. It has been proposed that CrFer1 functions to buffer the iron released as a consequence of the degradation of some Fe-containing proteins of the photosynthetic apparatus (Long et al., 2008). In Arabidopsis, ferritins have recently been shown to be necessary to prevent oxidative damage originating from the presence of free Fe in plastids when plants are exposed to excess Fe (Ravet et al., 2009a). In microorganisms, Mn plays a role in protection against oxidative stress (Anjem et al., 2009). During Mn deficiency, increased degradation of photosynthetic proteins leading to the release of free Fe or decreased Mn protective effect could lead to oxidative stress. The observed increase in ferritin levels could buffer iron and prevent oxidative damage.

Materials and methods

Plant material

The generation of the *nramp3-1* single mutant, the 35S-*AtNRAMP3* lines, the *nramp3nramp4* double mutant and the complemented lines *nramp3nramp4* AtNRAMP3 and *nramp3nramp4* AtNRAMP4 were described previously (Thomine et al., 2003; Lanquar et al., 2005).

Growth conditions

For perlite growth experiments, perlite (Puteaux fournitures horticoles, Les Clayes-sous-Bois, France) was washed once with 2.5 mM EGTA and then with about 10 volumes of deionized water. Arabidopsis seeds were sown on perlite and watered with a modified Hoagland's solution (0.28 mM KH_2PO_4, 1.25 mM KNO_3, 0.75 mM $MgSO_4$, 1.5 mM $Ca(NO3)_2$, 25 µM H_3BO_3, 50 µM KCl, 1 µM $ZnSO_4$, 0.1 µM Na_2MoO_4, 0.5 µM $CuSO_4$, 10 µM FeHBED, 3 mM MES-KOH, pH 5.7). Iron was provided as Fe^{3+} chelated to HBED (N,N'-di(2-hydroxybenzyl) ethylene diamine-N,N'-diacetic acid monochloride hydrate; Strem chemicals, Newburyport MA, USA). FeHBED was prepared as described (Lanquar et al., 2005). Plants were grown for 6 to 9.5 weeks with (C) or without 5 µM $MnSO_4$ (- Mn).

For the hydroponic growth experiments, seeds were surface sterilized and sown on bottom-cut 0.5 mL Eppendorf tubes filled with 0.8 % (w/v) Noble agar. For the first week, 6 seeds were placed in 500 mL of 0.5X Hoagland medium supplemented with 20 µM FeHBED and with (C and - Fe) or without 5 µM $MnSO_4$ (- Mn). Then, plants were grown either for 5 more weeks in 1X Hoagland medium supplemented with 10 µM FeHBED and with (C) or without 5 µM $MnSO_4$ (- Mn) or for 3 weeks in medium supplemented with 10 µM FeHBED, 5 µM $MnSO_4$ and then transferred into a medium supplemented with 5 µM $MnSO_4$ and 20 µM Ferrozine (- Fe) for 2 weeks. For culture on soil, on perlite or in hydroponics, plants were grown in a climate chamber, under the following conditions: 9/15h light/dark; light intensity 200 µE m^{-2} s^{-1}; constant temperature of 21°C; 60% rel. humidity).

Vacuole isolation

After removing the abaxial epidermis by rubbing on P600 sandpaper Arabidopsis leaves of plants grown on soil for 6 weeks, protoplasts were isolated by enzymatic

digestion of ~2 g of leaves in 50 mL MCP [500 mM Sorbitol, 1 mM $CaCl_2$, 10 mM MES, pH 5.6 (KOH)] supplemented with 0.03% (w/v) Pectolyase Y23 (Yakult Pharmaceuticals Ind.) and 0.75 % (w/v) Cellulase R10 (Yakult Pharmaceuticals Ind.) at 23°C for 2 h. Protoplasts were filtered through a 75-μm nylon mesh, pelleted (100g, 5 min) and washed twice with MCP; *ca.* 2 $x10^8$ protoplasts were obtained. Protoplasts were diluted to 15-20 x 10^6 cells mL^{-1}, and were lysed by addition of an equal volume of protoplast lysis buffer [200 mM Sorbitol, 10 % (w/v) Ficoll 400, 20 mM EDTA, 10 mM HEPES pH 8 (KOH), 0.15 % (w/v) BSA, 2 mM dithiothreitol (DTT)] prewarmed to 42°C. Protoplast lysis was monitored microscopically, and lysed protoplasts were kept on ice. Vacuoles were isolated and concentrated using a step gradient prepared on ice (1500 g, 20 min, 4°C): bottom phase, 1 volume of lysed protoplasts; middle phase, 0.8 volume of lysis buffer diluted in vacuole buffer to reach a concentration of 4 % (w/v) Ficoll; top phase, 0.2 volume of vacuole buffer [500 mM Sorbitol**,** 10 mM HEPES, pH 7.5 (KOH)**,** 0.15 % (w/v) BSA, 1 mM DTT, 2 μg mL^{-1} leupeptine, 2 μg mL^{-1} antipaine]. Vacuoles were recovered at the interface between the middle phase and the top phase. Purity of the vacuole preparation was monitored by microscopy; *ca.* 2 x 10^7 vacuoles were obtained in total.

For immunoblot analysis, after isolation, vacuoles were lysed as follows: 1 volume of vacuoles was mixed by inversion with 3 volumes of 50 mM MOPS pH 7.8, 0.1 mM DTT and 1X Complete Protease Inhibitor Cocktail Tablets (Roche Applied Science). The vacuolar membrane was collected by ultracentrifugation at 110,000 g at 4°C for 90 min, and the pellet was resuspended in the same MOPS-DTT buffer. Protein concentration was determined by the Bradford method.

Chloroplast isolation

Protoplasts were isolated and lysed as described above for the isolation of vacuoles. Percoll gradients were prepared by ultracentrifugation (40'000 g, 55 min, 4°C, without brake): bottom phase, 1 volume 100% Percoll; top phase: 1 volume of washing medium [300 mM Sorbitol, 40 mM TRICINE pH 7.6, 2.5 mM EDTA, 0.5 mM $MgCl_2$] and kept at 4°C. Chloroplasts were isolated by loading 6 ml of protoplast lysate on the preformed Percoll gradient followed by centrifugation (13'000 g, 10 min, 4°C, without brake). Intact chloroplasts were recovered at the bottom of the tube and were washed four times with cold washing medium (Ferro et al., 2002). Purity and integrity

of the chloroplast preparation was monitored by microscopy and the amount of chloroplasts was evaluated by measurement of the chlorophyll content.

Protein isolation

Total protein extracts from protoplasts, shoots and roots were prepared by homogenization in 50 mM HEPES NaOH pH 7.2, 1.5 mM $MgCl_2$, 1 mM EGTA, 1 mM EDTA, 10 % (w/v) Glycerol, 1 % (v/v) Triton-X100, 150 mM NaCl, 5 mM DTT and 1X Complete Protease Inhibitor Cocktail Tablets (Roche Applied Science). Samples were then centrifuged for 10 min, 1000 g at 4°C and supernatants were recovered. Protein concentration was estimated by the Bradford method.

Immunoblot analysis

Unless specified, 15 µg of vacuolar membrane, protoplast, root or shoot proteins were separated on SDS-PAGE and immunoblot analysis was performed. Rabbit anti-AtNRAMP3 polyclonal antibodies were raised against two synthetic peptides corresponding to N-terminal and C-terminal regions of AtNRAMP3 protein (N-term H2N-MPQLENNEP LLINEC-CONH2 ; C-term H2N-CTPWPFKAESSH–COOH) (Eurogentec). The anti-AtNRAMP3 antibodies were affinity-purified against the same peptides.

The antibodies used in this study were diluted as follows: AtNRAMP3 1:1000; AtNRAMP4 1:2000, AtVPPAse 1:20.000 dilution (Sarafian et al., 1992), AtFerritin 1:10.000 (Dellagi et al., 2005), AtIRT1 1/8000 (Seguela et al., 2008) PsbA/D1 1/15.000 (Agrisera, Sweden). Immunoblots were performed as described previously (Lanquar et al., 2005).

Metal content measurements

Leaves, shoots and roots were harvested separately and washed. Roots were desorbed by incubation in ice cold buffer containing 5 mM $CaCl_2$, 1 mM MES KOH pH 5.7 for 10 min. The dry biomass (DW) of the samples was measured after drying at 60^{o}C. Protoplast and vacuole samples were concentrated in a SpeedVac® after determination of the number of vacuoles or protoplasts per sample by counting objects under the microscope. All samples were digested in 65% nitric acid in a MARS5 microwave (CEM GmbH, Kamp-Lintford, Germany) at 200^{o}C at 15 bar for 10 min. After dilution in trace metal free water, the metal content of the samples was

determined by inductively coupled plasma atomic emission spectroscopy (ICP-AES) using an IRIS Advantage Duo ER/S (Thermo Jarrell Ash, Franklin, MA, USA) as described (Lanquar et al., 2005). The metal concentrations were expressed either as mg kg^{-1} DW for tissue samples, pg per object for protoplasts and vacuoles, or relative to the geometric mean of a combination of elements: Ca, Cu, Fe, Mg, Mn, Mo, P and Zn for protoplasts; Cu, P and S for chloroplasts. Note that other elements could not be used because of contaminant levels in the buffer in which chloroplasts were suspended.

Chlorophyll fluorescence measurements.

Room temperature chlorophyll fluorescence was measured *in vivo* using a pulse-amplitude modulation fluorimeter (PAM 101-3, Walz, Effeltrich). The intensity of the measuring light (standard PAM 101set) was sufficiently low (integral intensity about 10^{-8} mol quanta m^{-2} s^{-1}, frequency of modulated light: 1.6 kHz) to prevent the reduction of plastoquinone. Saturating flashes (1 s) were given to measure the maximum fluorescence. Efficiency of the photochemical electron transport was assayed by calculating the ratio of variable fluorescence Fv to maximal fluorescence Fm (Fv/Fm) (Maxwell and Johnson, 2000). In all experiments, the Fv/Fm ratio was measured on leaves of dark adapted plants. As photoinhibitory white light (Figure 4B), a cold light source was used with an intensity of 2000 µmol quanta m^{-2} s^{-1}. Recovery was followed for 3 h in dim white light (5 µmol quanta m^{-2} s^{-1}).

Thermoluminescence measurements

Thermoluminescence was measured with a home-built apparatus. To measure the thermoluminescence originating from the $S_{2/3}Q_B^-$ charge recombination (B band), excised leaf pieces were incubated in the dark at 20°C for 5 min and then flashed with saturation Xenon flashes at 1°C (1 s interval between flashes). Samples were heated with a constant rate (0.4°C s^{-1}) from 1°C to 70°C and the light emission was recorded. Graphical and numerical data analyses were performed as described (Ducruet and Miranda, 1992).

Superoxide dismutase activity

Total leaf protein extracts were prepared by homogenization in 100 mM potassium phosphate pH 7, 3.5 mM DTT, 1 mM EDTA, 1 mM PMSF, 15% (v/v) glycerol, 1%

(w/v) PVP (polyvinylpyrrolidone), 0.1% (v/v) Triton X-100. Samples were centrifuged (10'000 g, 5 min, 4°C) and supernatants were recovered. Protein concentration was estimated by the Bradford method. Total protein extracts were separated on a native polyacrylamide gel (12%, Precast Gel, BioRad, USA) and SOD activity was detected in gel as described (Beauchamp and Fridovitch, 1971). FeSOD and CuZnSOD activities were identified by sensitivity to 2 mM KCN for CuZnSOD and sensitivity to 5 mM H_2O_2 for CuZnSOD and FeSOD. Treatments were performed prior to activity staining.

Supplemental material

Supplemental figure 1: characterization of an anti-AtNRAMP3 polyclonal antibody.

Supplemental figure 2: rescue of the *nramp3nramp4* growth defect in the absence of manganese by *AtNRAMP3* or *AtNRAMP4*.

Supplemental figure 3: phenotype and metal content of *nramp3nramp4* plants grown in hydroponic culture.

Supplemental figure 4: time course variations of Fv/Fm in wild type, *nramp3*, *nramp4* and *nramp3nramp4* under Mn sufficient or deficient conditions.

Supplemental figure 5: quantification of D1 immunoblot and silver staining as loading control.

Supplemental table 1: metal concentrations of wild-type and *nramp* mutant rosettes, grown in presence (control) or absence of manganese (- Mn)

Supplemental table 2: chlorophyll fluorescence of complemented *nramp3nramp4* plants.

Acknowledgements

The authors thank Drs F. Gaymard and C. Curie for sharing FER1 and IRT1 antibodies before publication.

Literature cited

Allen MD, Kropat J, Tottey S, Del Campo JA, Merchant SS (2007) Manganese deficiency in Chlamydomonas results in loss of photosystem II and MnSOD function, sensitivity to peroxides, and secondary phosphorus and iron deficiency. Plant Physiol **143:** 263-277

Anjem A, Varghese S, Imlay JA (2009) Manganese import is a key element of the OxyR response to hydrogen peroxide in *Escherichia coli*. Mol Microbiol **72:** 844-858

Baxter IR, Vitek O, Lahner B, Muthukumar B, Borghi M, Morrissey J, Guerinot ML, Salt DE (2008) The leaf ionome as a multivariable system to detect a plant's physiological status. Proc Natl Acad Sci U S A **105:** 12081-12086

Beauchamp C, Fridovitch I (1971) Superoxide dismutase: improved assays and an assay applicable to acrylamide gels. Anal. Biochem. **44:** 276-287

Björkman O, Demmig B (1987) Photon yield of O_2 evolution and chlorophyll fluorescence characteristics at 77 K among vascular plants of diverse origins Planta **170:** 489-504

Bondarava N, De Pascalis L, Al-Babili S, Goussias C, Golecki JR, Beyer P, Bock R, Krieger-Liszkay A (2003) Evidence that cytochrome b559 mediates the oxidation of reduced plastoquinone in the dark. J Biol Chem **278:** 13554-13560

Briat JF, Lobreaux S, Grignon N, Vansuyt G (1999) Regulation of plant ferritin synthesis: how and why? Cell Mol Life Sci **56:** 155-166

Carter C, Pan S, Zouhar J, Avila EL, Girke T, Raikhel NV (2004) The vegetative vacuole proteome of *Arabidopsis thaliana* reveals predicted and unexpected proteins. Plant Cell **16:** 3285-3303

Colangelo EP, Guerinot ML (2006) Put the metal to the petal: metal uptake and transport throughout plants. Curr Opin Plant Biol **9:** 322-330

Connolly EL, Fett JP, Guerinot ML (2002) Expression of the IRT1 metal transporter is controlled by metals at the levels of transcript and protein accumulation. Plant Cell **14:** 1347-1357

Curie C, Alonso JM, Le Jean M, Ecker JR, Briat JF (2000) Involvement of NRAMP1 from *Arabidopsis thaliana* in iron transport. Biochem. J. **347:** 749-755

Delhaize E, Gruber BD, Pittman JK, White RG, Leung H, Miao Y, Jiang L, Ryan PR, Richardson AE (2007) A role for the AtMTP11 gene of Arabidopsis in manganese transport and tolerance. Plant J **51:** 198-210

Delhaize E, Kataoka T, Hebb DM, White RG, Ryan PR (2003) Genes encoding proteins of the cation diffusion facilitator family that confer manganese tolerance. Plant Cell **15:** 1131-1142

Dellagi A, Rigault M, Segond D, Roux C, Kraepiel Y, Cellier F, Briat JF, Gaymard F, Expert D (2005) Siderophore-mediated upregulation of Arabidopsis ferritin expression in response to *Erwinia chrysanthemi* infection. Plant J **43:** 262-272

Ducruet JM, Miranda T (1992) Graphical and numerical analysis of thermoluminescence and fluorescence F0 emission in photosynthetic material. Photosynth Res **33:** 15-27

Ferro M, Salvi D, Riviere-Rolland H, Vermat T, Seigneurin-Berny D, Grunwald D, Garin J, Joyard J, Rolland N (2002) Integral membrane proteins of the chloroplast envelope: identification and subcellular localization of new transporters. Proc Natl Acad Sci U S A **99:** 11487-11492

González A, Lynch J (1999) Subcellular and tissue Mn compartmentation in bean leaves under Mn toxicity stress. Aust J Plant Physiol **26:** 811–822

Hebbern CA, Laursen KH, Ladegaard AH, Schmidt SB, Pedas P, Bruhn D, Schjoerring JK, Wulfsohn D, Husted S (2009) Latent manganese deficiency increases transpiration in barley (*Hordeum vulgare*). Physiol Plant **135:** 307-316

Hirschi KD, Korenkov VD, Wilganowski NL, Wagner GJ (2000) Expression of arabidopsis CAX2 in tobacco. Altered metal accumulation and increased manganese tolerance. Plant Physiol **124:** 125-133

Husted S, Laursen KH, Hebbern CA, Schmidt SB, Pedas P, Haldrup A, Jensen PE (2009) Manganese deficiency leads to genotype-specific changes in fluorescence induction kinetics and state transitions. Plant Physiol **150:** 825-833

Ifuku K, Yamamoto Y, Ono TA, Ishihara S, Sato F (2005) PsbP protein, but not PsbQ protein, is essential for the regulation and stabilization of photosystem II in higher plants. Plant Physiol **139:** 1175-1184

Inoue Y (1996) Photosynthetic thermoluminescence as a simple probe of photosystem II electron transport. *In* J Amesz, AJ Hoff, eds, Biophysical techniques in photosynthesis. Kluwer academic publishers, Netherlands, pp 93-107

Kim SA, Punshon T, Lanzirotti A, Li L, Alonso JM, Ecker JR, Kaplan J, Guerinot ML (2006) Localization of iron in Arabidopsis seed requires the vacuolar membrane transporter VIT1. Science **314:** 1295-1298

Koren'kov V, Park S, Cheng NH, Sreevidya C, Lachmansingh J, Morris J, Hirschi K, Wagner GJ (2006) Enhanced Cd^{2+}-selective root-tonoplast-transport in tobaccos expressing Arabidopsis cation exchangers. Planta **225:** 403-411

Korshunova YO, Eide D, Clark WG, Guerinot ML, Pakrasi HB (1999) The IRT1 protein from *Arabidopsis thaliana* is a metal transporter with a broad substrate range. Plant Mol Biol **40:** 37-44

Lanquar V, Lelièvre F, Barbier-Brygoo H, Thomine S (2004) Regulation and function of AtNRAMP4 metal transporter protein. Soil Sci. Plant Nutr. **50:** 1141-1150

Lanquar V, Lelièvre F, Bolte S, Hames C, Alcon C, Neumann D, Vansuyt G, Curie C, Schroder A, Kramer U, Barbier-Brygoo H, Thomine S (2005) Mobilization of vacuolar iron by AtNRAMP3 and AtNRAMP4 is essential for seed germination on low iron. EMBO J **24:** 4041-4051

Liu XF, Culotta VC (1999) Post-translation control of Nramp metal transport in yeast. Role of metal ions and the *BSD2* gene. J. Biol. Chem. **274:** 4863-4868

Long JC, Sommer F, Allen MD, Lu SF, Merchant SS (2008) FER1 and FER2 encoding two ferritin complexes in *Chlamydomonas reinhardtii* chloroplasts are regulated by iron. Genetics **179:** 137-147

Luk EE, Culotta VC (2001) Manganese superoxide dismutase in *Saccharomyces cerevisiae* acquires its metal co-factor through a pathway involving the Nramp metal transporter, Smf2p. J Biol Chem **276:** 47556-47562

Makui H, Roig E, Cole ST, Helmann JD, Gros P, Cellier MF (2000) Identification of the *Escherichia coli* K-12 Nramp orthologue (MntH) as a selective divalent metal ion transporter. Mol. Microbiol. **35:** 1065-1078

Marschner H (1995) Mineral Nutrition of Higher Plants. Academic Press, London

Maxwell K, Johnson GN (2000) Chlorophyll fluorescence--a practical guide. J Exp Bot **51:** 659-668

Mills RF, Doherty ML, Lopez-Marques RL, Weimar T, Dupree P, Palmgren MG, Pittman JK, Williams LE (2008) ECA3, a Golgi-localized P2A-type ATPase, plays a crucial role in manganese nutrition in Arabidopsis. Plant Physiol **146:** 116-128

Nevo Y, Nelson N (2006) The NRAMP family of metal-ion transporters. Biochim Biophys Acta **1763:** 609-620

Oomen RJ, Wu J, Lelièvre F, Blanchet S, Richaud P, Barbier-Brygoo H, Aarts MG, Thomine S (2009) Functional characterization of NRAMP3 and NRAMP4

from the metal hyperaccumulator *Thlaspi caerulescens*. New Phytol **181:** 637-650

Patzer SI, Hantke K (2001) Dual repression by Fe^{2+}-Fur and Mn^{2+}-MntR of the mntH gene, encoding an NRAMP-like Mn^{2+} transporter in *Escherichia coli*. J Bacteriol **183:** 4806-4813

Pedas P, Hebbern CA, Schjoerring JK, Holm PE, Husted S (2005) Differential capacity for high-affinity manganese uptake contributes to differences between barley genotypes in tolerance to low manganese availability. Plant Physiol **139:** 1411-1420

Pedas P, Ytting CK, Fuglsang AT, Jahn TP, Schjoerring JK, Husted S (2008) Manganese efficiency in barley: identification and characterization of the metal ion transporter HvIRT1. Plant Physiol **148:** 455-466

Peiter E, Montanini B, Gobert A, Pedas P, Husted S, Maathuis FJ, Blaudez D, Chalot M, Sanders D (2007) A secretory pathway-localized cation diffusion facilitator confers plant manganese tolerance. Proc Natl Acad Sci U S A **104:** 8532-8537

Pittman JK (2005) Managing the manganese: molecular mechanisms of manganese transport and homeostasis. New Phytol **167:** 733-742

Pittman JK, Shigaki T, Marshall JL, Morris JL, Cheng NH, Hirschi KD (2004) Functional and regulatory analysis of the Arabidopsis thaliana CAX2 cation transporter. Plant Mol Biol **56:** 959-971

Portnoy ME, Liu XF, Culotta VC (2000) *Saccharomyces cerevisiae* expresses three functionally distinct homologues of the nramp family of metal transporters. Mol. Cell. Biol. **20:** 7893-7902

Que Q, Helmann JD (2000) Manganese homeostasis in *Bacillus subtilis* is regulated by MntR, a bifunctional regulator related to the diphtheria toxin repressor family of proteins. Mol. Microbiol. **35:** 1454-1468

Quiquampoix H, Loughman BC, Ratcliffe RG (1993) Quantitative Aspects of the ^{31}P-NMR Detection of Manganese in Plant Tissues J. Exp. Bot. **44:** 1809-1818

Ravet K, Touraine B, Boucherez J, Briat JF, Gaymard F, Cellier F (2009a) Ferritins control interaction between iron homeostasis and oxidative stress in Arabidopsis. Plant J **57:** 400-412

Ravet K, Touraine B, Kim SA, Cellier F, Thomine S, Guerinot ML, Briat JF, Gaymard F (2009b) Post-Translational Regulation of AtFER2 Ferritin in Response to Intracellular Iron Trafficking during Fruit Development in Arabidopsis. Mol Plant **2:** 1095-1106

Rutherford AW, Crofts AR, Inoue Y (1982) Thermoluminescence as a probe of photosystem II photochemistry: the origin of the flash-induced glow peaks. Biochim Biophys Acta **682:** 457-465

Sarafian V, Kim Y, Poole RJ, Rea PA (1992) Molecular cloning and sequence of cDNA encoding the pyrophosphate-energized vacuolar membrane proton pump of *Arabidopsis thaliana*. Proc Natl Acad Sci U S A **89:** 1775-1779

Segond D, Dellagi A, Lanquar V, Rigault M, Patrit O, Thomine S, Expert D (2009) NRAMP genes function in *Arabidopsis thaliana* resistance to *Erwinia chrysanthemi* infection. Plant J **58:** 195-207

Seguela M, Briat JF, Vert G, Curie C (2008) Cytokinins Negatively Regulate the Root Iron Uptake Machinery in Arabidopsis through a growth-dependent pathway. Plant J **55:** 289-300

Thomine S, Lelièvre F, Debarbieux E, Schroeder JI, Barbier-Brygoo H (2003) AtNRAMP3, a multispecific vacuolar metal transporter involved in plant responses to iron deficiency. Plant J. **34:** 685-695

Thomine S, Wang R, Ward JM, Crawford NM, Schroeder JI (2000) Cadmium and iron transport by members of a plant metal transporter family in *Arabidopsis* with homology to Nramp genes. Proc. Natl. Acad. Sci. USA. **97:** 4991-4996

Vert G, Grotz N, Dedaldechamp F, Gaymard F, Guerinot ML, Briat JF, Curie C (2002) IRT1, an *Arabidopsis* transporter essential for iron uptake from the soil and for plant growth. Plant Cell **14:** 1223-1233

Wada S, Ishida H, Izumi M, Yoshimoto K, Ohsumi Y, Mae T, Makino A (2009) Autophagy plays a role in chloroplast degradation during senescence in individually darkened leaves. Plant Physiol **149:** 885-893

White PJ, Bowen HC, Demidchik V, Nichols C, Davies JM (2002) Genes for calcium-permeable channels in the plasma membrane of plant root cells. Biochim Biophys Acta **1564:** 299-309

Wu Z, Liang F, Hong B, Young JC, Sussman MR, Harper JF, Sze H (2002) An endoplasmic reticulum-bound Ca^{2+}/Mn^{2+} pump, ECA1, supports plant growth and confers tolerance to Mn^{2+} stress. Plant Physiol **130:** 128-137

Figure Legends

Figure 1: AtNRAMP3 and AtNRAMP4 proteins reside on mesophyll vacuoles and are involved in the control of vacuolar Mn content.

(A) Immunoblot analysis of proteins from leaves, mesophyll protoplasts and mesophyll vacuoles from wild-type and *nramp3nramp4* mutant plants. The blots were probed with an anti-NRAMP3, an anti-NRAMP4 antibody or an antibody raised against the vacuolar membrane pyrophosphatase (V-PPase).

(B) Fe, Mn and Zn concentrations in leaves (left), protoplasts (middle) and vacuoles (right) measured by ICP-AES. Grey bars: wild type, white bars: *nramp3nramp4*. Leaf metal concentration is expressed as $\mu g.g^{-1}$; protoplast and vacuole metal contents are expressed as pg per object. Mean ± s.e. n = 6 independent experiments for the protoplast preparations; n = 7 independent experiments for vacuole. * and *** denote significant differences based on Mann Whitney U-test between genotypes with $p < 0.05$ (*) and $p < 0.001$ (***) respectively.

In A and B, plants were grown on soil for 6 weeks.

Figure 2: Arabidopsis *nramp3nramp4* plants display a growth reduction in the absence of manganese supply in the medium which is rescued by expression of *AtNRAMP3* or *AtNRAMP4* genes.

Plants were grown on perlite for 8 weeks (A, D) or 9.5 weeks (B, C) on control medium (5 µM Mn) or - Mn medium (0 µM Mn). (A) Photographs of wild-type and *nramp3nramp4* rosettes. (B) Leaves of wild type and *nramp3nramp4*. Left: younger leaves; right: older leaves. (C) Fresh biomass of wild-type (WT), *nramp3* (*nr3*), *nramp4* (*nr4*) and *nramp3nramp4* (*nr3nr4*) rosettes. Mean value ± s.e. (n = 10-20) plants for each genotype in each condition). (D) Fresh biomass of wild-type (WT), *nramp3nramp4* (*nr3nr4*), *nramp3nramp4 AtNRAMP3* (*nr3nr4*+NR3) and *nramp3nramp4 AtNRAMP4* (*nr3nr4*+NR4) rosettes. Mean value ± s.e. (n = 12-24 plants for each genotype in each condition). Different letters denote a statistically significant difference ($p < 0.01$ based on Kruskal Walis test for multiple comparisons).

Figure 3: Mn concentration in leaves and mesophyll protoplasts is equal or higher in *nramp3nramp4* than in wild type.

Wild-type (grey bars) or *nramp3nramp4* (white bars) plants were grown on perlite for leaf metal concentration measurements and in hydroponic condition for protoplast relative metal concentrations under control (C: 5 µM Mn) or Mn deficient (- Mn) for 8 weeks.

(A) Mean ± s.e. of Fe, Mn and Zn concentrations of leaves from plants grown on perlite (*n* = 3 samples containing each 10 leaves from 3-4 plants).

(B) Mean ± s.e. of Fe, Mn and Zn relative concentrations of protoplast from plants grown under hydroponic conditions (*n* = 3 protoplast preparations from independent biological replicates). Results are expressed as relative units (R.U.): Fe, Mn and Zn metal content were normalized to the geometric mean of all other reliably measured element contents (Ca, Cu, Fe, Mg, Mn, Mo, P and Zn). Note that expressing the results as metal content / protoplast yielded similar results.

Asterisks indicate statistically significant differences between wild type and *nramp3 nramp4* mutant (Mann Whitney U-test, $p < 0.01$).

Figure 4: PSII activity and chloroplast Mn content are altered in Mn deficient *nramp3nramp4* plants.

(A) Intensity of thermoluminescence signals recorded from excised leaf pieces of dark-adapted manganese-deficient wild-type and *nramp3nramp4* plants grown on perlite for 8 weeks under Mn deficient conditions. Black and grey squares represent the amplitude in arbitrary units (a.u.) of the TL (Thermo Luminescence) B band in wild-type and *nramp3nramp4* leaf segments, respectively. Series of zero to eight single turnover flashes were given at 1°C after 5 min of dark adaptation of the leaf segment at 20°C. Similar results were obtained in 2 independent biological replicates.

(B) Fluorescence recovery after photoinhibition measured on attached leaves of double mutant (left) and wild-type (right) plants grown on perlite for 8 weeks under Mn deficient conditions. Upper panel: plants grown in the absence of Mn (- Mn), lower panel: plants grown in control conditions (C: 5 µM Mn). Open arrows: onset/termination of the measuring light; closed arrows: onset/termination of the actinic light (white light at 2000 µmol quanta $m^{-2}s^{-1}$); dim light (6 µmol quanta $m^{-2}s^{-1}$). Similar results were obtained in 2 independent biological replicates.

(C) D1 (PsbA) protein levels in leaves of wild-type or *nramp3nramp4* plants analyzed by immunoblot (higher panel). Five, 2.5, 1.25 and 0.62 μg total leaf proteins from 9.5 week old plants grown on perlite under control (C: 5 μM Mn) or Mn deficient (- Mn) conditions were loaded. Silver staining of proteins on gels run in parallel indicate that equal amounts of proteins were loaded (lower panel). Similar results were obtained in 3 independent biological replicates.

(D) Relative Mn concentrations of intact chloroplasts isolated from wild-type (grey bars) or *nramp3nramp4* (white bars) plants grown under control (C: 5 μM Mn) or Mn deficient (- Mn) for 8 weeks in hydroponic conditions. Mn concentrations were normalized to the geometric mean of all other reliably measured element concentrations (Cu, P and S). Note that additional elements could not be used for normalization because of their concentrations in the chloroplast suspension buffer. Results are expressed as mean ratio ± s.e. taking the Mn content in chloroplast from wild-type plants grown under control conditions as reference (*n* = 3 independent biological replicates).

Figure 5: MnSOD activity is maintained in *nramp3nramp4* Mn deficient leaves.

In-gel SOD activity staining was performed in the absence (A) or in the presence of 5 mM H_2O_2 (B). Hundred micrograms of total leaf proteins from 9.5 week old plants grown on perlite under control (C: 5 μM Mn), Fe deficient (- Fe) or Mn deficient (- Mn) were separated by native PAGE before activity staining. Similar results were obtained with 2 independent biological replicates.

Figure 6: AtNRAMP3 and AtNRAMP4 protein levels are not regulated in response to Mn deficiency but ferritins are accumulated in shoots of Mn-deficient *nramp3nramp4* plants.

(A) AtNRAMP3 and AtNRAMP4 protein levels in roots and shoots of wild-type plants analyzed by immunoblot. Extracts of root and shoot proteins from *nramp3nramp4* plants grown on control medium were loaded as a negative control.

(B) Ferritin and IRT1 protein levels were monitored by immunoblot on *nramp3nramp4* and wild-type plants. The FER1 antibody was used on blots of shoot extracts and the IRT1 antibody was used on blots of root extracts.

In A and B, 15 µg total proteins from roots or shoots of plants grown for 6 weeks under hydroponic conditions were analyzed. Mn deficient plants were grown without added Mn in the growth medium for 6 weeks. To induce Fe deficiency, after 4 weeks, plants were transferred in a medium containing 20 µM Ferrozine in the absence of added Fe for 2 more weeks.

Table I: Rosette fresh biomass and chlorophyll fluorescence of 8-week-old wild-type and *nramp3nramp4* plants grown on perlite in presence (control: 5 µM Mn) or absence of manganese (- Mn). Results shown correspond to mean ± s.e. with *n* number of plants weighted and *n'* number of Fv/Fm measurements on different leaves. Results from one representative experiment out of 5. Mann-Whitney U-test, $^{**}p < 0.01$, $^{*}p < 0.05$, $^{\triangle}p > 0.05$.

	Fresh biomass (*n*)	Fv/Fm (*n'*)
Control medium		
Wild type	537 ± 69 (11)	0.798 ± 0.003 (10)
nramp3nramp4	582 ± 92$^{\Delta}$ (6)	0.796 ± 0.004$^{\Delta}$ (12)
- Mn medium		
Wild type	279 ± 36 (15)	0.655 ± 0.013 (11)
nramp3nramp4	82 ± 24** (10)	0.572 ± 0.017* (9)

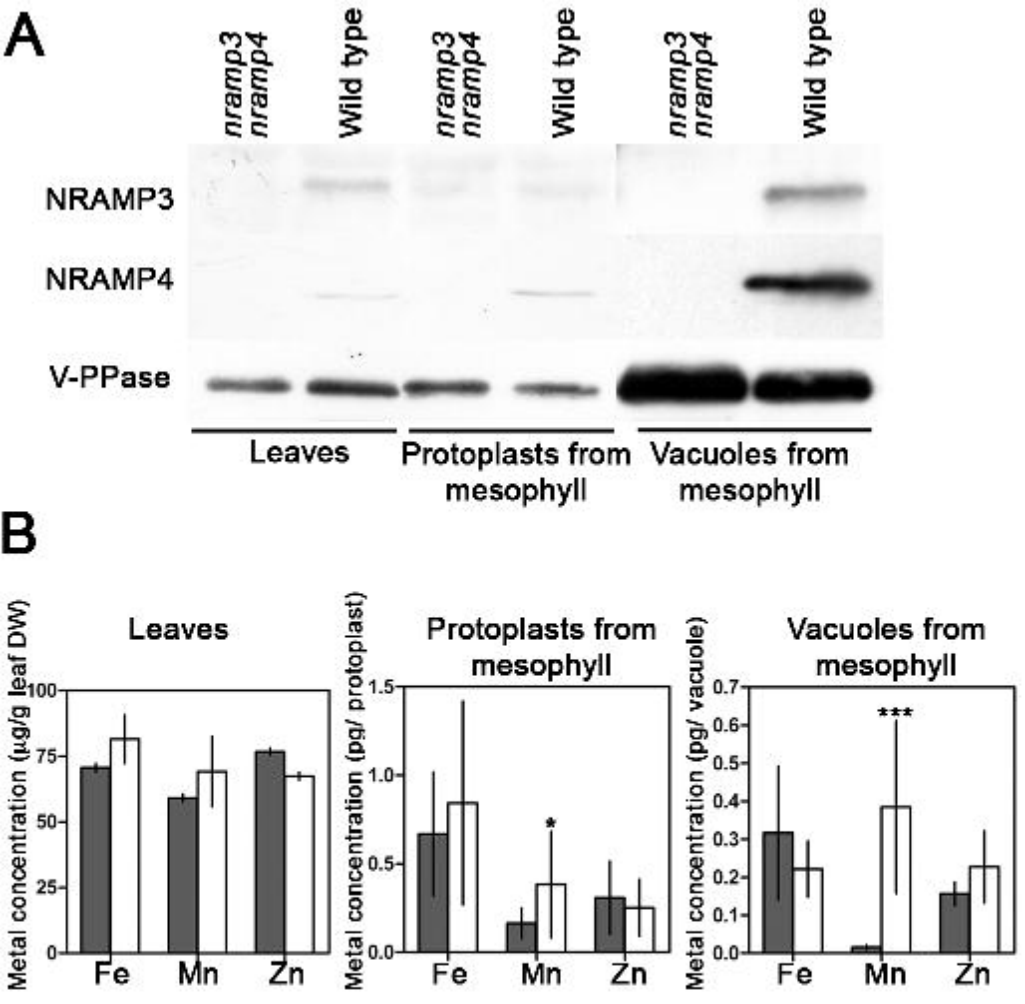

Figure 1
Lanquar *et al*

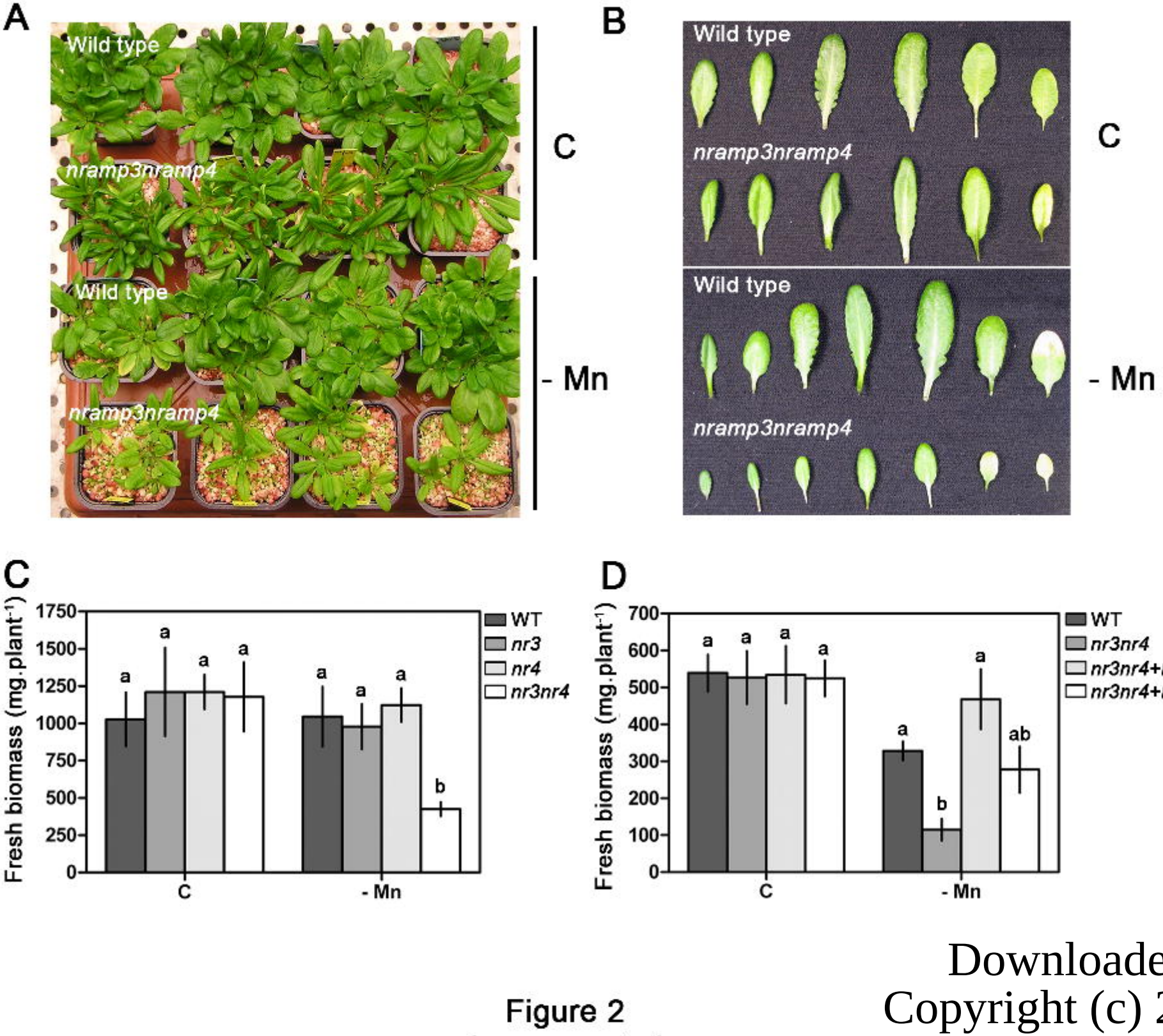

Figure 2
Lanquar *et al*

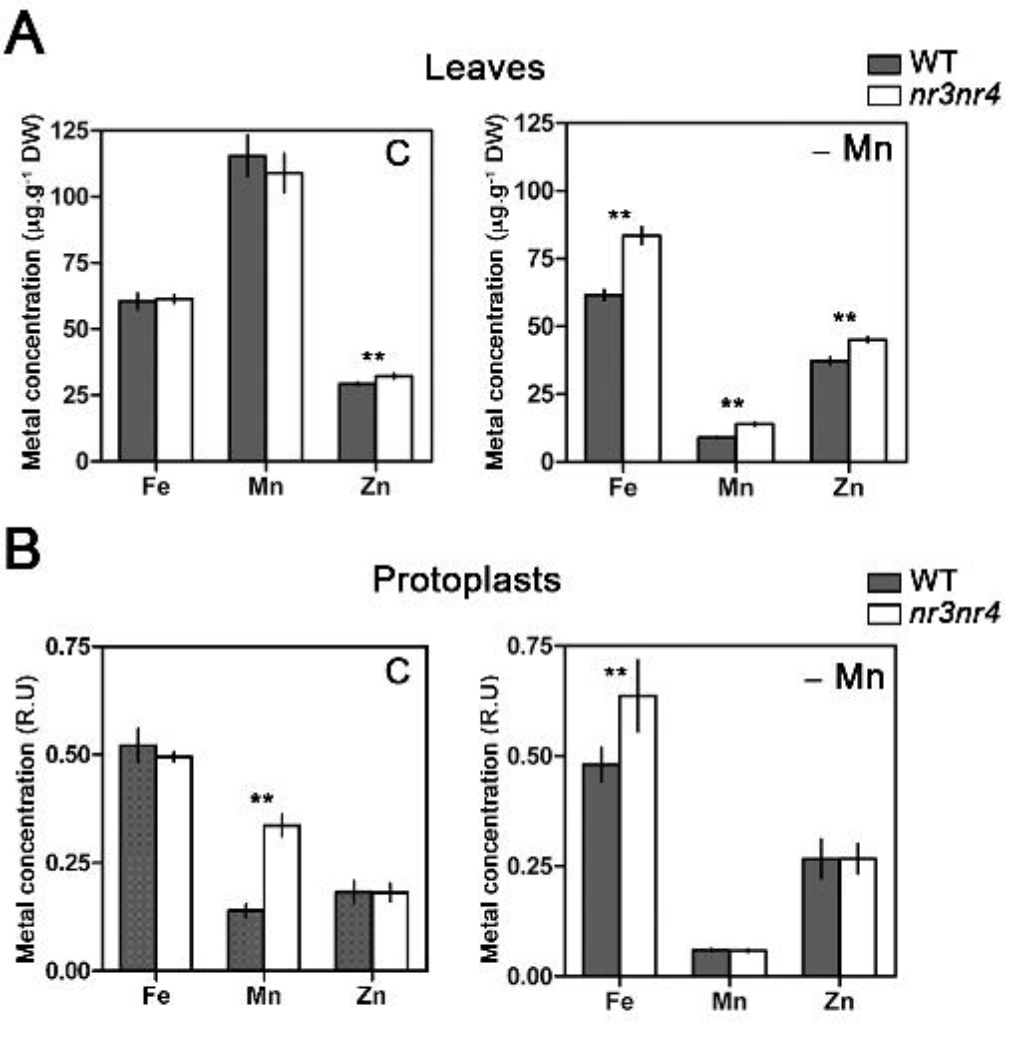

Figure 3
Lanquar *et al*

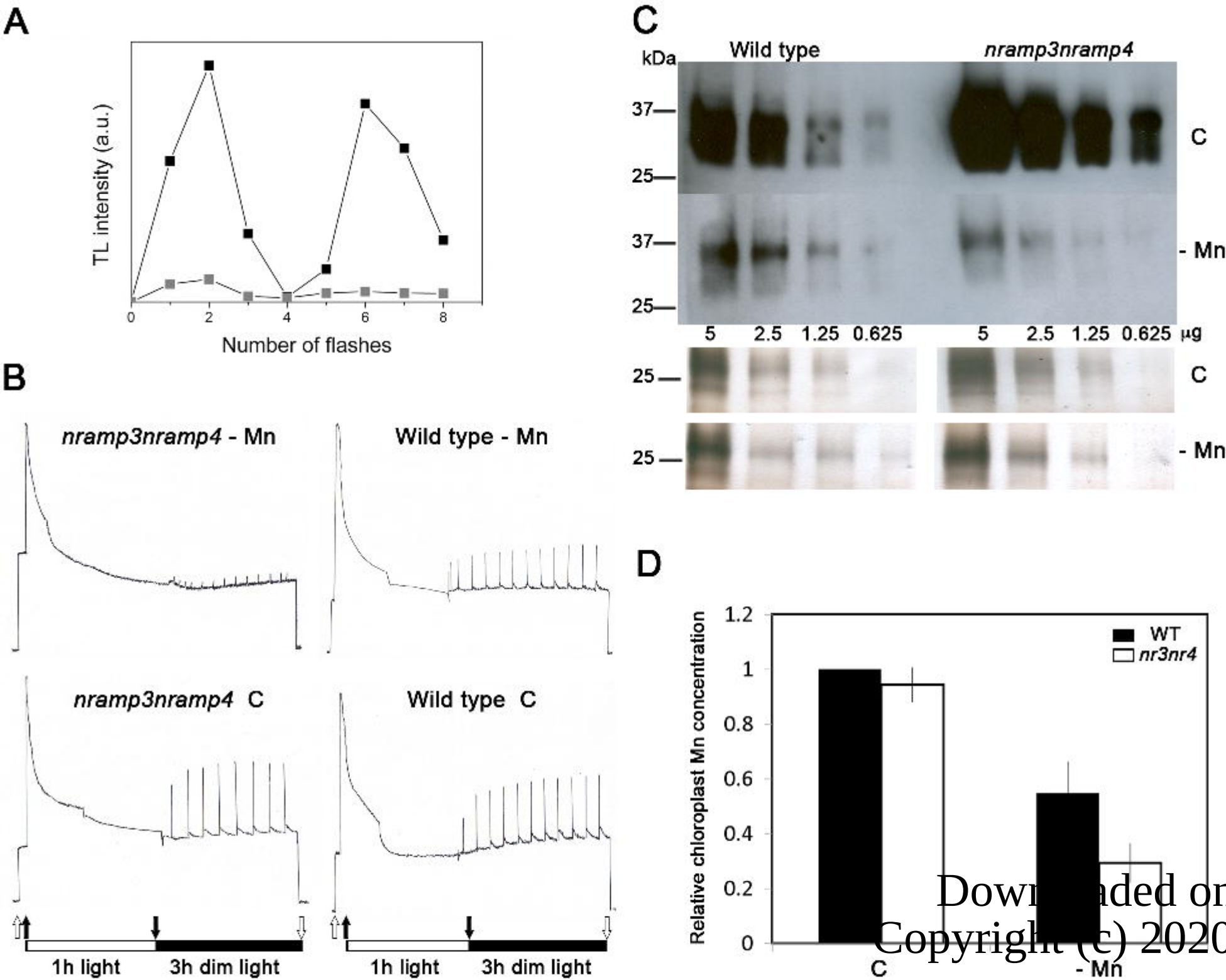

Figure 4
Lanquar *et al*

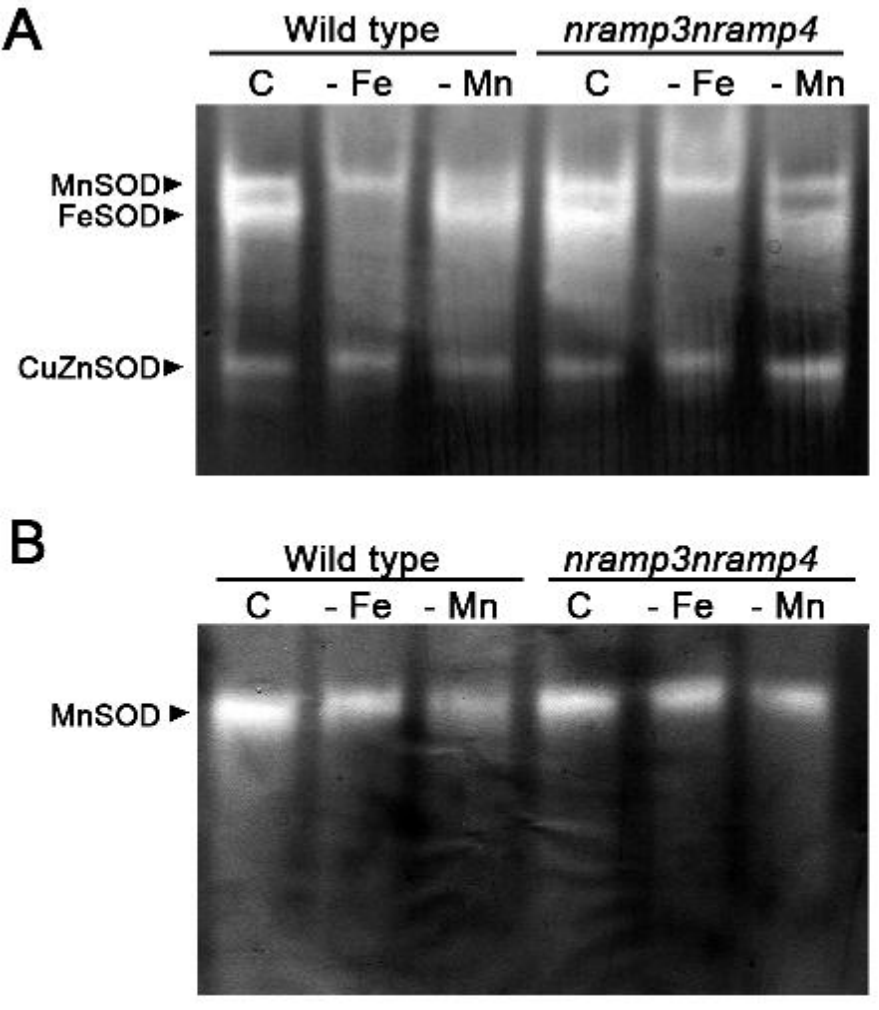

Figure 5
Lanquar *et al*

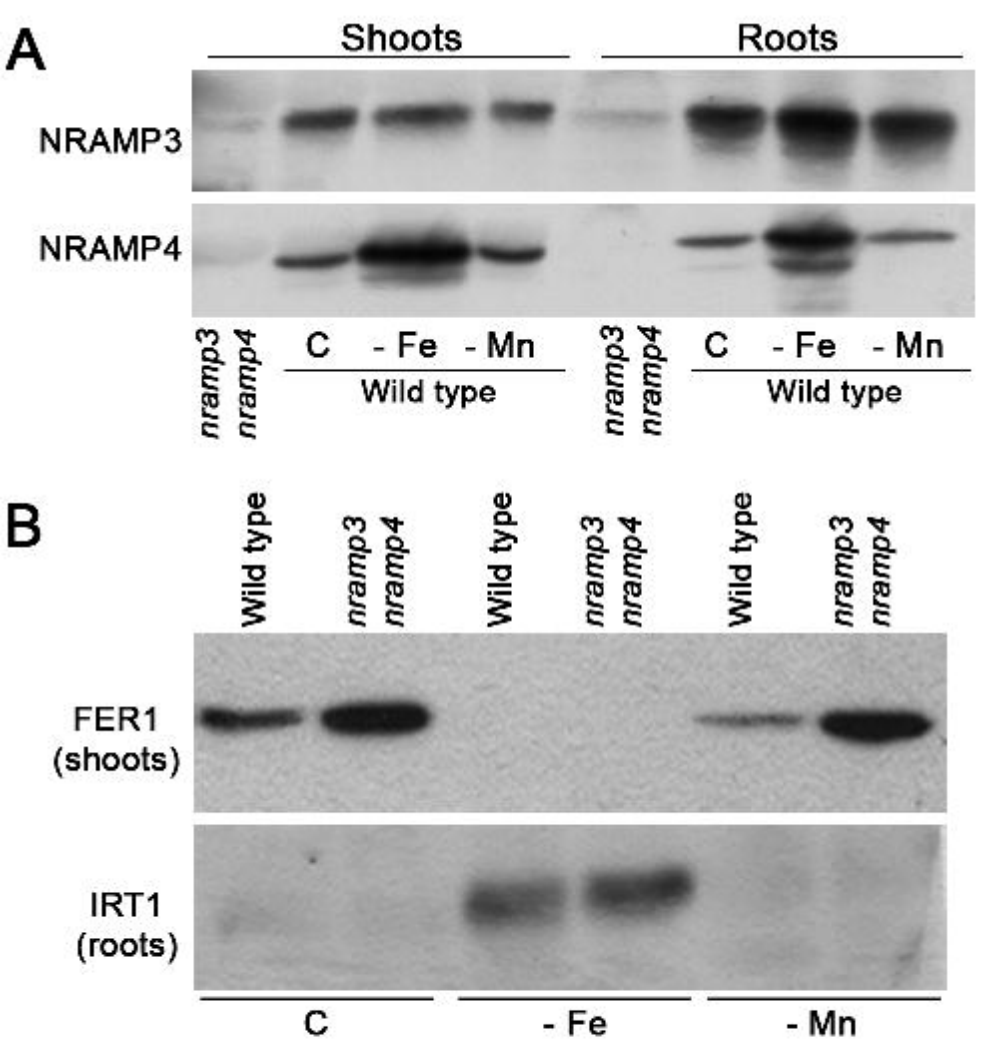

Figure 6
Lanquar *et al*